24th COBEM - 2017

24thABCM International Congress of Mechanical Engineering
December 3-8, 2017, Curitiba, PR, Brazil

COBEM-2017-1383
NUMERICAL ANALYSIS OF GFRP POLES

Plínio Ricardo dos Santos
Carlos Alberto Cimini Junior
Universidade Federal de Minas Gerais, Av. Pres. Antônio Carlos, 6627 - Pampulha, Belo Horizonte - MG, 31270-901
plinioricardosantos@hotmail.com
cimini@ufmg.br

Abstract. *Poles have an important purpose in the distribution of electrical energy. Other sectors such as the telephone and internet also use this means to bring their services to homes. Currently, the poles are made of wood, reinforced concrete, and steel. However, these materials are subject to problems such as rapid wood degradation, high weight and difficult positioning for reinforced concrete poles and corrosion in steel. Some alternatives are adopted to minimize these problems, such as wood treatment, optimization of concrete structures and protection of steel surfaces. Another alternative is to look for new types of materials to supply all pole requirements. Composite materials, such as glass fiber-reinforced polymer (GFRP), have great advantages because they are resistant, light and insulating. Monocoque and semi-monocoque structures, commonly used in aircraft fuselages, allow reduction in final mass, which combined with the use of composite materials generate even lighter structures (in the case of poles, up to seven times lighter). In this work, monocoque and semi-monocoque structures configurations were analyzed, using longitudinal stiffeners and transverse rings, in different combinations. The finite difference method was used for the calculation of the maximum deflection for the purpose of evaluatingthe stiffness adequately. Global and local buckling and failure were also evaluated. Abaqus™ commercial finite element software was used to obtain the results.*

Keywords: *Poles; Composite Material; GFRP; Monocoque; Semi-monocoque.*

1. INTRODUCTION

The poles are traditionally made of wood, steel or concrete reinforced with steel. However, there are some disadvantages about the use of these materials. Use of wood, for example, generates limitation in final height, besides being decomposed by the attack of fungi and bacteria. Poles made of concrete are heavier, leading to transport and positioning problems. Steel also offers greater weight, and in addition, it has corrosion problems (Metiche and Masmoudi, 2012). These are some of the problems that have made manufacturers and researchers seek other alternatives for the design and the use of galvanizing or paints for steel (Birchal, 2001). Another alternative is the search for new materials that meet conditions imposed on the electrical system.

The purpose of this work was to analyse poles in monocoque and semi-monocoque configurations using GFRP materials. The maximum allowable deflection at the pole end was preliminarily determined using the finite difference method (FDM). Then, the commercial software Abaqus™, based on the finite element method (FEM) was used to analyse the structural stability and material failure.

2. PROCEDURES

2.1 Pole characteristic

Figure 1a shown a pole draw, where the main elements are named. Outer skin is an element that resists mainly the shear and can be manufactured by filament winding method (Cimini, *et al.*, 2005). Longitudinal stringers (cross section is shown in Figure 1b) are produced by pultrusion method and resists mainly axial and bending. Both the skin and stringers are made with GFRP. The rings (Figure 1c) have the purpose of resisting local buckling and are made with wood. Material constitutive properties for the GFRP composite (Table 1) were obtained from Fam, *et al.* (2010) and for the wood used in rings, the properties (Table 2) were obtained from Pfeil (2013). The diameters of the base and the top of the pole are respectively 500 mm and 250 mm, while the total height is 12 m, with 1.8 m of grounding.

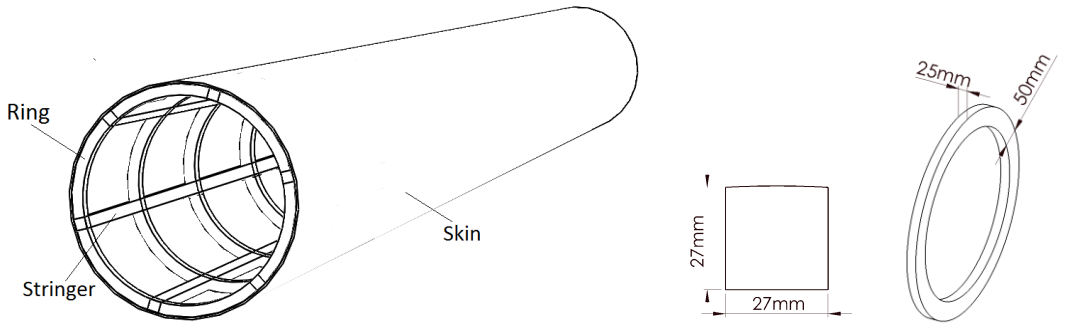

(a) (b) (c)

Figure 1: (a) Pole components; (b) Stringer cross section; (c) Ring geometry

Table 1: GFRP composite properties

ρ (kg/m³)	E_1 (MPa)	E_2 (MPa)	υ_{12}	G_{12} (MPa)	F_{1t} (MPa)	F_{1c} (MPa)	F_{2t} (MPa)	F_{2c} (MPa)	F_{12} (MPa)
2540	43300	11900	0.24	4600	1020	-620	40	-140	60

Table 2: Wood properties

ρ (kg/m³)	fc (Mpa)	ft (Mpa)	ftn (Mpa)	fv (Mpa)	Ec (Mpa)
999.00	62.00	123.00	3.90	10.70	18421.00

In Tables 1 and 2: E_1 is modulus of elasticity parallel to filament; E_2 is modulus of elasticity transverse to filament; υ_{12} is the Poisson's ratio; G_{12} is shear modulus in 12 plane; F_{1t} is tension stress allowable parallel to filament; F_{1c} is compression stress allowable parallel to filament; F_{2t} is tension stress allowable transverse to filament; F_{2c} is compression stress allowable transverse to filament and F_{12} is shear stress allowable in 12 plane; ρ is material density; f_c is compression stress allowable parallel to fibers; f_t is tension stress allowable parallel to fibers; f_{tn} is tension stress allowable normal to fibers; f_v is shear stress allowable and E_c is modulus of elasticity parallel to fibers.

2.2 Numerical Model

The Finite Differences Method is a numerical way to approximate the solution of differential equations using the Taylor series. Soares (2010) evaluated the convergence of this method applied to the Bernoulli-Euler beams theory, obtaining results with great precision. According to Cunha (2000), to apply the method, we must first discretize the region. The nodal displacement is given by Equation 1 (Soares, 2010), implemented in Matlab® software.

$$\begin{pmatrix} w_1 \\ w_2 \\ w_3 \\ w_4 \\ w_5 \\ \vdots \\ w_{n-3} \\ w_{n-2} \\ w_{n-1} \\ w_n \end{pmatrix} = \begin{pmatrix} 0 & 2 & 0 & 0 & 0 & 0 & & & & & \\ 0 & -2 & 1 & 0 & 0 & 0 & & & & & \\ 0 & 1 & -2 & 1 & 0 & 0 & \cdots & & & \cdots & \\ 0 & 0 & 1 & -2 & 1 & 0 & & & & & \\ 0 & 0 & 0 & 1 & -2 & 1 & & & & & \\ & & & \vdots & & & \ddots & & \vdots & & \\ & & & & & & & 1 & -2 & 1 & 0 & 0 \\ & & & & & & & 0 & 1 & -2 & 1 & 0 \\ & & & \cdots & & & \cdots & 0 & 0 & 1 & -2 & 1 \\ & & & & & & & 0 & 0 & 0 & 0 & 0 \end{pmatrix}^{-1} \begin{pmatrix} C_1 \\ C_2 \\ C_3 \\ C_4 \\ C_5 \\ \vdots \\ C_{n-3} \\ C_{n-2} \\ C_{n-1} \\ C_n \end{pmatrix} \quad (1)$$

where:

$$C_i = \frac{h^2 M_i}{E_i I_i} \quad (2)$$

h is the distance between two neighboring nodes;

M is the bending moment;
E is elasticity module;
I is the moment of inertia;
i is the point analyzed.

To analyze the structural stability, or buckling, the commercial software Abaqus®, based on the finite element method, was used. Thus, the problem of eigenvalues is solved, shown by Equation 3, which estimates the critical buckling load (bifurcation) of the structure (Dassault Systèmes, 2010).

$$\left(\boldsymbol{K}_0^{NM} + \lambda_j \boldsymbol{K}_\Delta^{NM}\right) v_j^M = 0 \tag{3}$$

where:

$\boldsymbol{K}_0^{NM}$ is the stiffness matrix corresponding to the base state, which includes the effects of the preloads;
$\boldsymbol{K}_\Delta^{NM}$ is the differential initial stress and load stiffness matrix due to the incremental loading pattern;
λ_j are the critical buckling (eigenvalues);
v_j^M are the buckling mode shapes (eigenvectors);
M e N refer to degrees of freedom M and N of the whole model;
j refers to the jth buckling mode.

The maximum strain failure criterion for composite materials was used in Abaqus™ software to analyze material failure. The failure occurs when at least one of the strain components along the principal material axes exceeds the corresponding ultimate strain in that direction (Daniel and Ishai, 2006). The Abaqus™ software computes the failure index, I_F, or *MSTRN*, defined by maximum ratio between the strain in the pole and the strain failure, in that respective directions, as presented in Equation 4 (Barbero, 2013).

$$I_F = \max\begin{cases} \varepsilon_1/\varepsilon_{1t} \quad if\ \varepsilon_1 > 0 \quad or \quad -\varepsilon_1/\varepsilon_{1c}\ if\ \varepsilon_1 < 0 \\ \varepsilon_2/\varepsilon_{2t} \quad if\ \varepsilon_2 > 0 \quad or \quad -\varepsilon_2/\varepsilon_{2c}\ if\ \varepsilon_2 < 0 \\ \varepsilon_3/\varepsilon_{3t} \quad if\ \varepsilon_3 > 0 \quad or \quad -\varepsilon_3/\varepsilon_{3c}\ if\ \varepsilon_3 < 0 \\ abs(\gamma_4)/\gamma_{4u} \\ abs(\gamma_5)/\gamma_{5u} \\ abs(\gamma_6)/\gamma_{6u} \end{cases} \tag{4}$$

where

ε is axial and transverse strain;
γ is shear strain.
The quantities in the numerator are the strain in the pole and the quantities in the denominator are the ultimate strains. The number index means the direction and the letters *t* and *c* means traction and compression, respectively. *max* and *abs* mean the maximum and absolute value, respectively.

The horizontal and vertical loads used were, respectively, Rn = 10000.00 N and Rv = 3825.90 N, and the maximum allowed deflection was 5% of the nominal length (CEMIG, 2010). Figure 2 shown Boundary condition applied in Abaqus™ model. The pole was clamped in the base and loads were applied 100 mm bellow the top. The model element size is 7 mm according to the convergence test. The rings and stringers were modeled using the beam elements B31, which has two nodes, and skin was modeled with quadrilateral shell elements S4R, constituted of four nodes, with the number of integrations reduced.

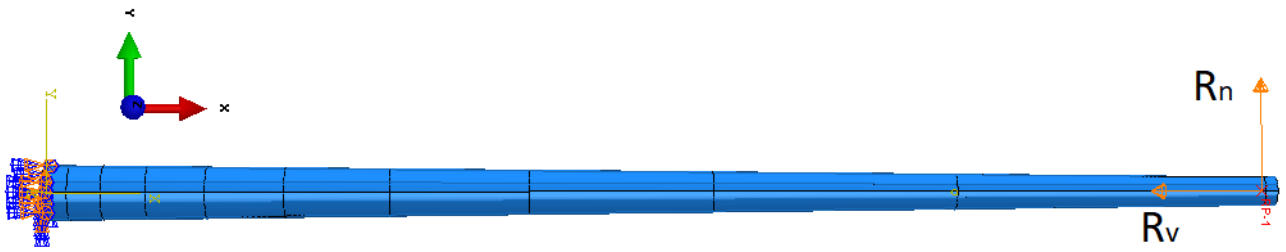

Figure 2: Boundary condition applied in Abaqus™ model

3. RESULTS AND DISCUSSIONS

The maximum deflection of the pole is one of the most important criteria of the analysis. The implementation of the DFM adjusted the stiffness and facilitated the analysis via FEM. The maximum deflection was set to a maximum 5% of total pole height. This maximum value of deflection has been maintained for all configurations for comparison. The numerical simulation for the critical buckling loads and strain failure index are shown in Figures 3 to 10. The analysis of the failure criterion for the maximum strain is done only for the skin in the Abaqus software, thus, to analyze the stringers, the maximum strain in the stringers direction was analyzed separately (Figures 7 and 9). All the configurations and results are summarized in the Table 3.

The configuration *A* (monocoque) presented the highest critical load, 195.12 kN and the lowest failure index, 0.2992 (Figures 3 and 4, respectively). However, this configuration presented the highest mass, 673.45 kg and presented a global buckling for the first mode, as show in Figure 3.

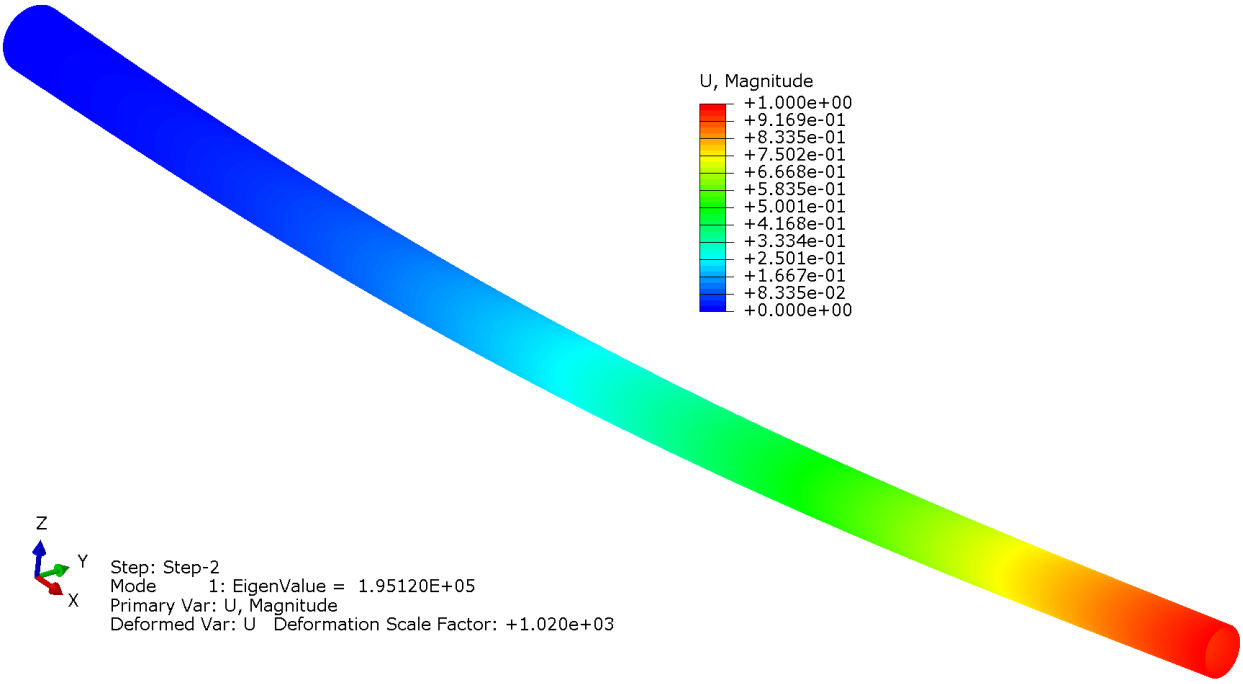

Figure 3: Buckling analysis for pole *A*

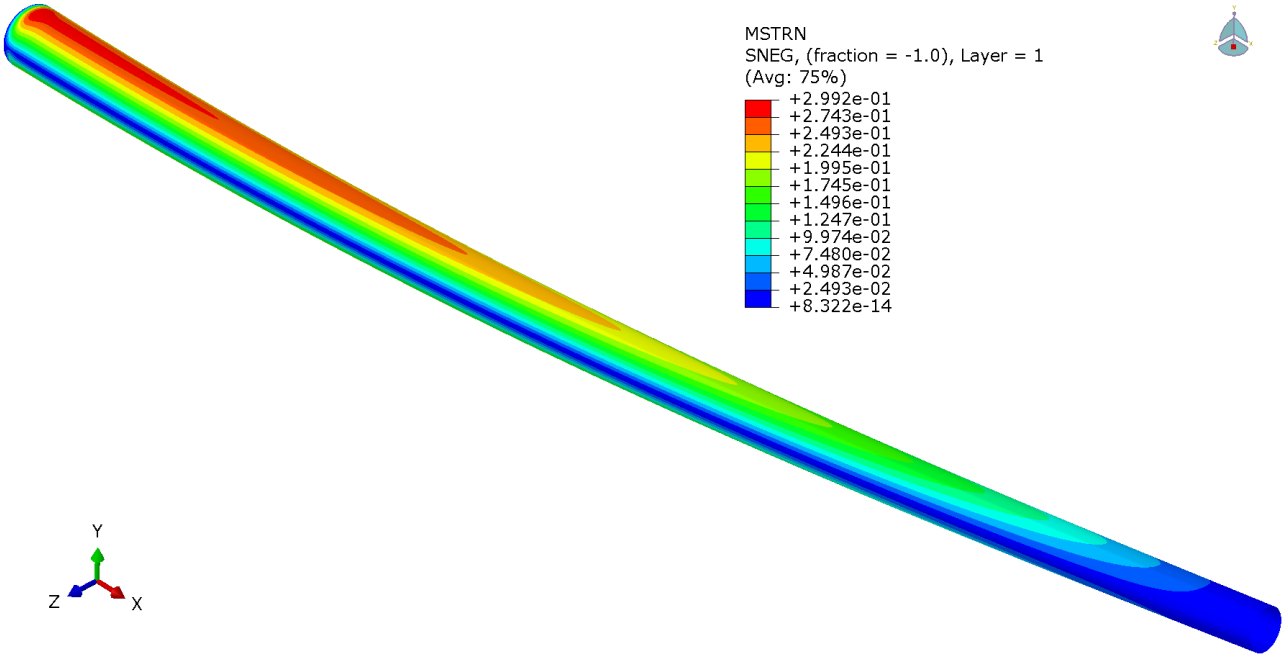

Figure 4: Strain failure index for pole *A*

The configuration *B* (semi-monocoque with eight stringers) presented the lowest critical load and mass, 44.58 kN and 358,41kg, respectively, and intermediary index failure, 0.4236 (Figure 6). For this case, there was local buckling near the base and the maximum deflection occurred in the regions of the stringers. The behavior is shown in Figure 5.

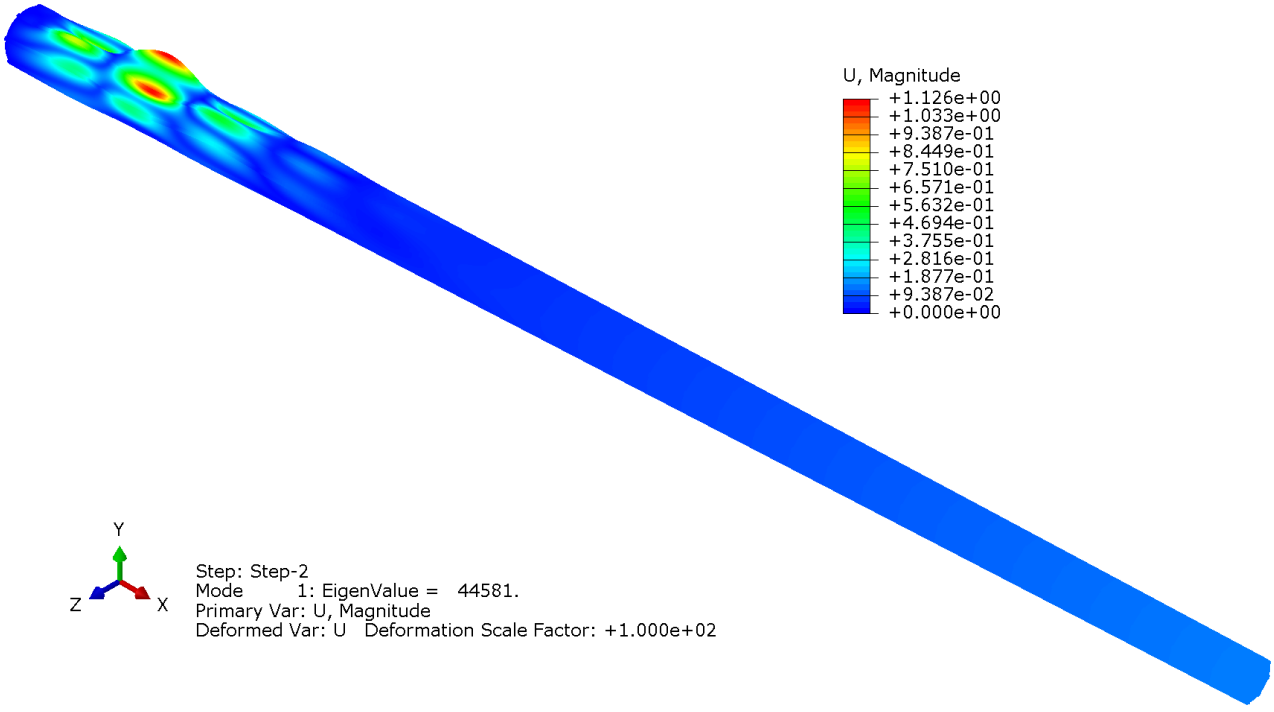

Figure 5: Buckling analysis for pole B

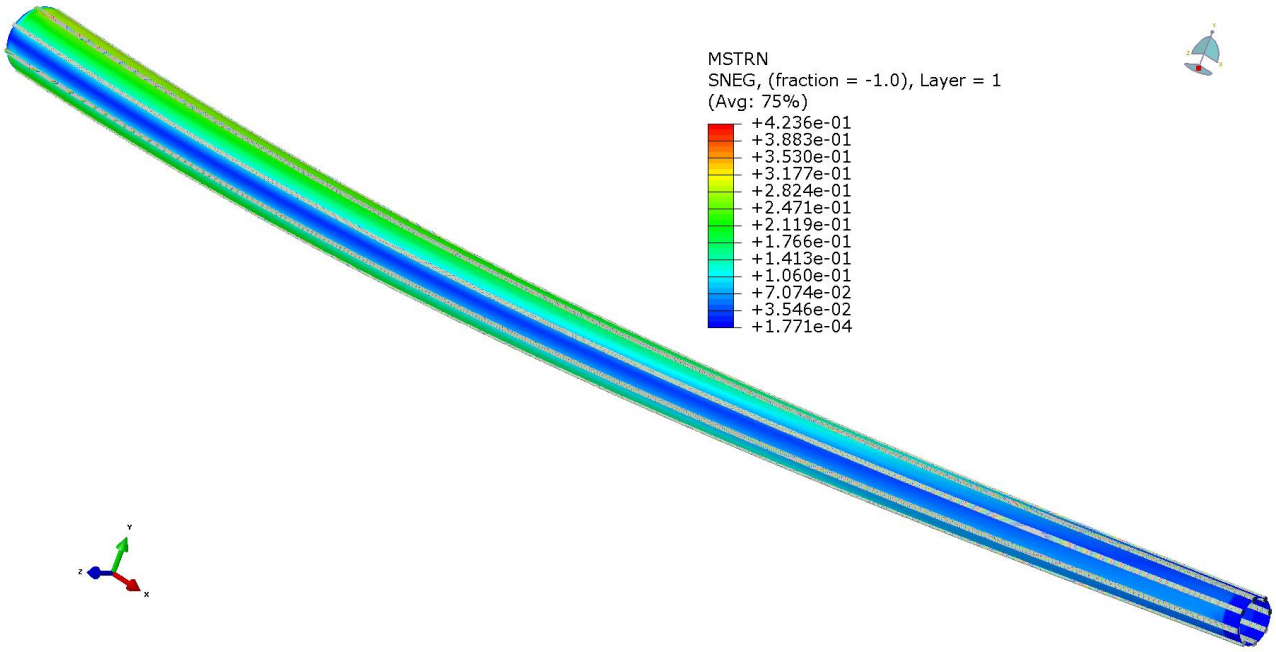

Figure 6: Strain failure index for pole B

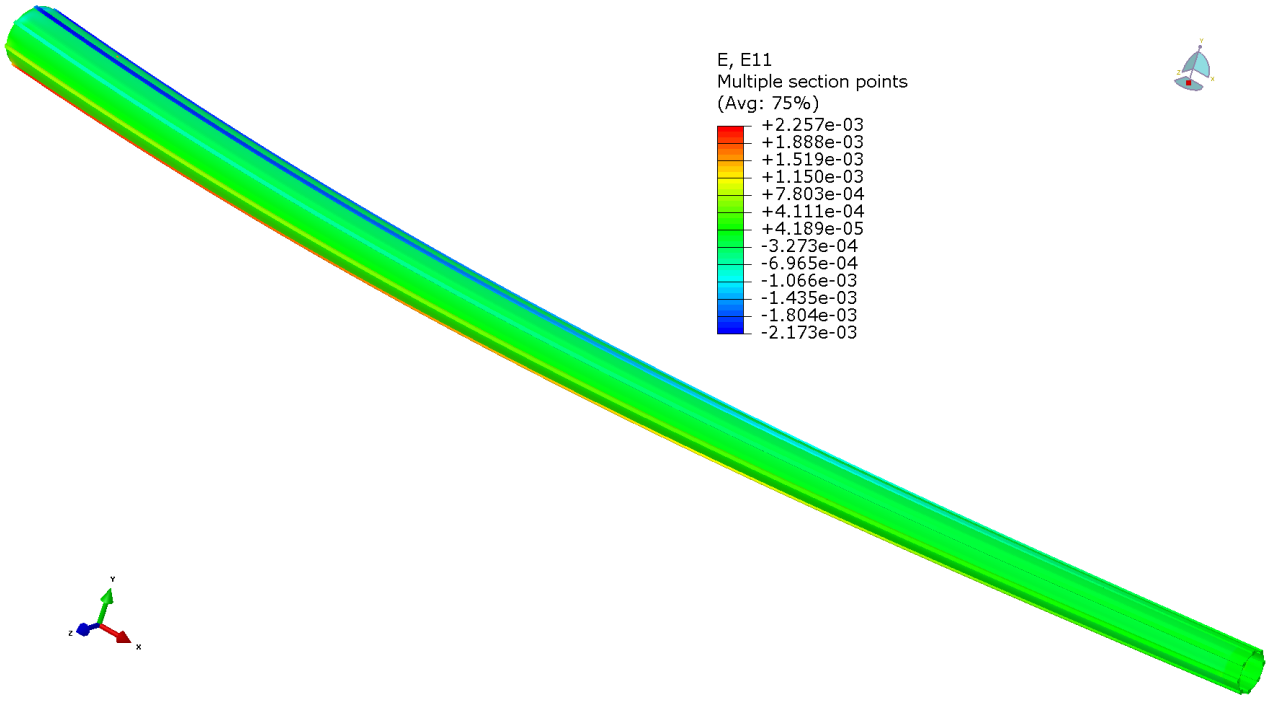

Figure 7: Longitudinal strain analysis for pole B

Analyzing the configuration *C* (semi-monocoque with eight stringers and ten rings), we can see that the addition of rings restricted the deflection of the skin and the stringers in the regions of the rings, which generated a higher critical buckling load and mass, 50.56 kN and 396.86 kg, respectively, than configuration *B*. Figure 8 in shown the behavior for the first mode of buckling. This configuration presented a failure index equal to 0.4408 (see Figure 10).

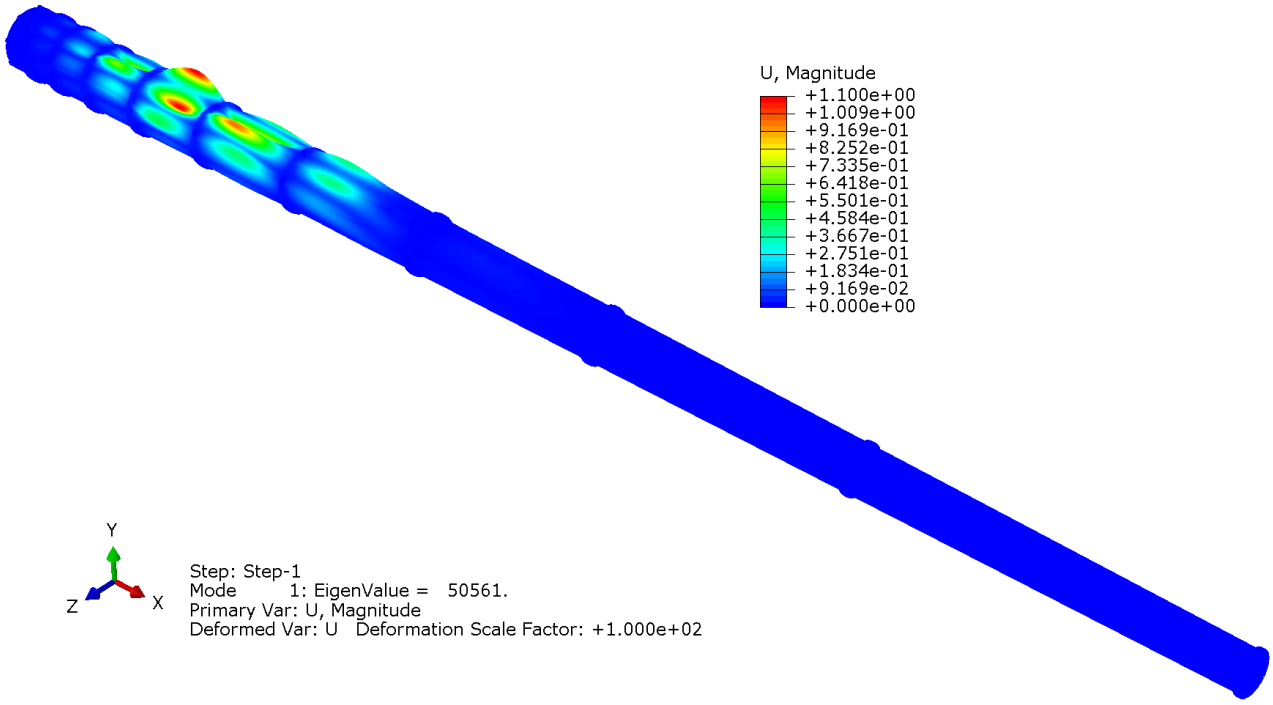

Figure 8: Buckling analysis for pole *C*

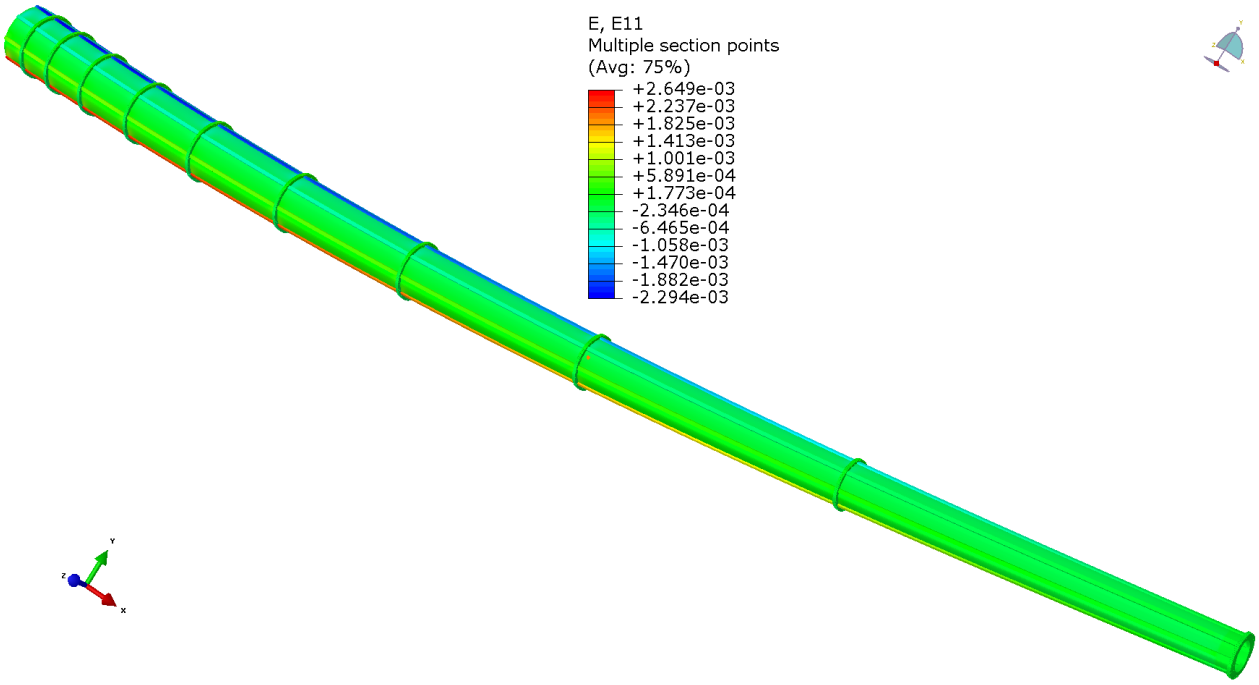

Figure 9: Longitudinal strain analysis for pole *C*

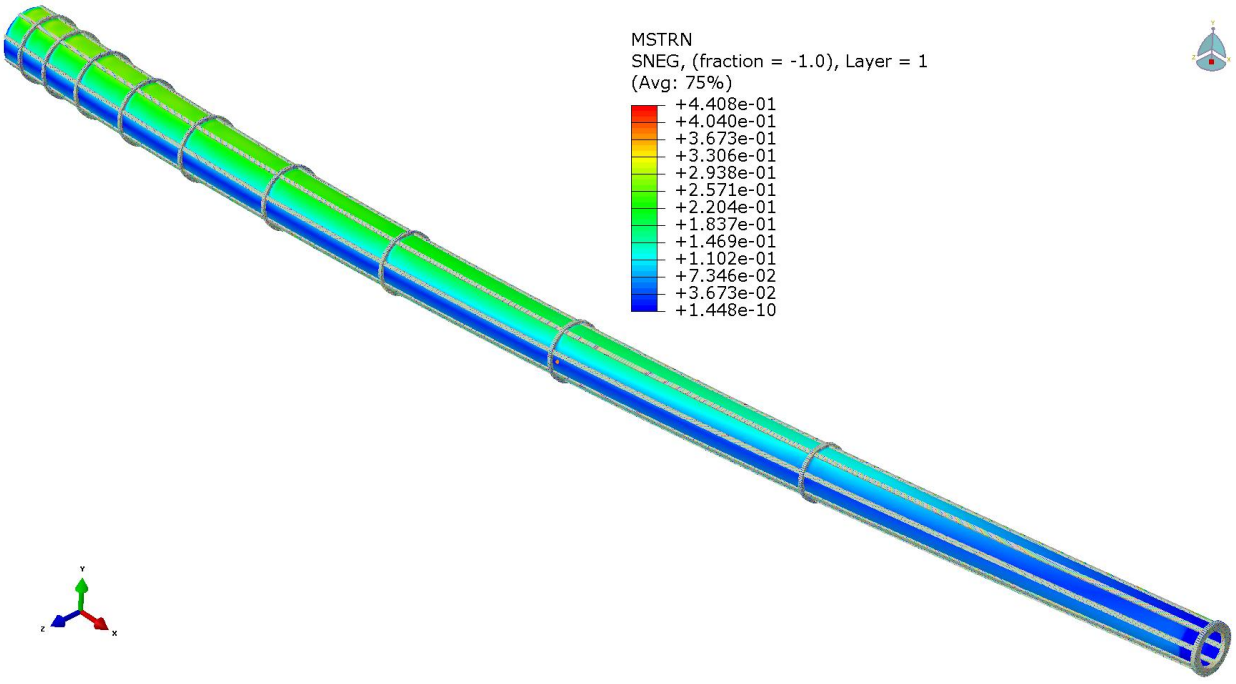

Figure 10: Strain failure index for pole *C*

Table 3: Deflection, critical load, mass and failure index results

Conditions	Stringers	Rings	Skin Thickness (mm)	Critical Load (kN)	Mass (kg)	I_F
A	without	without	19.8	195.12	673.45	0.2992
B	8	without	5.1	44.58	358,41	0.4236
C	8	10	5.1	50.56	396.86	0.4408

4. CONCLUSIONS

Monocoque and semi-monocoques poles were analyzed. Configuration *A* presented the highest mass and highest critical load. When the stringers were added (pole *B* and *C*) there was an increase in pole stiffness for thinner skin thicknesses. The *C* configuration had the mass and critical buckling loading intermediate due to addition of the rings and restriction of the buckling length. The configurations *B* and *C* presented close failure indexes and the configuration *A* presented the lowest failure index.

This work will contribute to future applications of the studied poles, thus allowing a rapid dimensioning of poles reinforced by fibers, more specifically glass fibers. The study presents the feasibility of design, fabrication and structural performance. Thus, future poles will facilitate the applications, mainly due to their good physical characteristics, allowing easy design, manufacturing, transportation and positioning, especially in rural areas difficult to access.

5. ACKNOWLEDGEMENTS

The authors gratefully acknowledge the important support of the Brazilian research agency FAPEMIG (in portuguese “Fundação de Amparo à Pesquisa do Estado de Minas Gerais”).

6. REFERENCES

Alípio, L.G.S.; Projeto e análise de postes de estrutura semi-monocoque fabricados com materiais compósitos. Belo Horizonte, 2014. 64p.Trabalho de conclusão de curso.

Barbeiro, E. J., 2013. The finite element analysis of composite materials using Abaqus™.

Birchal, G.A.; Postes autoportantes em materiais compostos poliméricos. Belo Horizonte, 2001. 144p. Dissertação de mestrado – Escola de Engenharia – Universidade Federal de Minas Gerais.

Cimini Jr, C.A., Meneses, H.R., Sobreira, A.E.C., Las Casas, E.B.,2005. "Experimental Analysis of GFRP Poles. *International Conference on Composite Materials-ICCM 15*, Durban, S. Africa.

Companhia Energética de Minas Gerais, 2010. "Especificação Técnica – Poste em Compósito (poste de poliéster reforçado com fibra de vidro – PRFV)".

Cunha, M.C., *Métodos Numéricos*, 2ª edição, Editora da Unicamp, Campinas, 2000 p.174

Daniel, I.M. and Ishai, O., *Engineering mechanics of composite materials*, Oxford University Press, Oxford, 2006

Dassault Systèmes, 2010. Abaqus Analysis User's Manual.

Fam, A.; Kim Y.J.; Son, J.K., 2010. A numerical investigation into the response of free end tubular composite poles subjected to axial and lateral loads, p.651-659

Metiche, L.; Masmoudi, R.; Analysis and design procedures for the flexural behavior of glass fiber-reinforced polymer composite poles. *Journal of Composite Materials*. 21, fevereiro, 2012. P. 207-208.

Pfeil, W. Pefeil, M., 2013. Estruturas de madeira: dimensionamento segundo a norma brasileira NBR 7190/97 e critérios das normas norte americana NDS e europeia EUROCODE 5, 6ª ed. Editora LTC, Rio de Janeiro. p.192.

Soares, A.A.B., 2010; O método das diferenças aplicado à teoria de vigas. Belém,. 126p.

7. RESPONSIBILITY NOTICE

The authors are the only responsible for the printed material included in this paper.